Proteomics Approach to Identify Dehydration Responsive Nuclear Proteins from Chickpea (*Cicer arietinum* L.)*Ⓢ

Aarti Pandey, Subhra Chakraborty‡, Asis Datta, and Niranjan Chakraborty§

Dehydration or water-deficit is one of the most important environmental stress factors that greatly influences plant growth and development and limits crop productivity. Plants respond and adapt to such stress by altering their cellular metabolism and activating various defense machineries. Mechanisms that operate signal perception, transduction, and downstream regulatory events provide valuable information about the underlying pathways involved in environmental stress responses. The nuclear proteins constitute a highly organized, complex network that plays diverse roles during cellular development and other physiological processes. To gain a better understanding of dehydration response in plants, we have developed a comparative nuclear proteome in a food legume, chickpea (*Cicer arietinum* L.). Three-week-old chickpea seedlings were subjected to progressive dehydration by withdrawing water and the changes in the nuclear proteome were examined using two-dimensional gel electrophoresis. Approximately 205 protein spots were found to be differentially regulated under dehydration. Mass spectrometry analysis allowed the identification of 147 differentially expressed proteins, presumably involved in a variety of functions including gene transcription and replication, molecular chaperones, cell signaling, and chromatin remodeling. The dehydration responsive nuclear proteome of chickpea revealed a coordinated response, which involves both the regulatory as well as the functional proteins. This study, for the first time, provides an insight into the complex metabolic network operating in the nucleus during dehydration. *Molecular & Cellular Proteomics 7:88–107, 2008.*

Environmental stress limits growth, development, and crop productivity (1, 2) and plays a major role in determining the geographic distribution of plant species. Several environmental stresses are united by the fact that at least part of their detrimental effect on plant performance is caused by disruption of plant water status. Periods of little or no rainfall can lead to a meteorological condition called drought. However, water deficit or dehydration, can also occur at conditions in which water is not limiting, through altered ion content and water uptake caused by high salinity or by formation of extracellular ice during freezing. Desiccation is the extreme form of dehydration wherein most of the protoplasmic "free" water is lost and the cell survival relies on the 'bound' water associated with the cell matrix. Dehydration is one of the most common environmental stresses to which plants are exposed, and in many regions it is the bottleneck of agricultural development (3). There is hardly a physiological process in plants that is not impaired by water deficit or dehydration. However, very few plants have been subjected to biochemical and molecular studies to analyze the mechanisms of dehydration stress tolerance. It appears that the intrinsic ability of plant to tolerate stress is a result of different biochemical and molecular mechanisms, and the elucidation of the nature of these mechanisms would be an interesting area of research. The stress perception and signal transduction to switch on adaptive responses are critical steps in determining the survival of plants exposed to adverse environments. Based on the presence of general and specific stress tolerance mechanisms (4), it is logical to expect plants to have multiple stress perception and signal transduction pathways, which may cross-talk at various steps. The alteration of protein synthesis or degradation is one of the fundamental metabolic processes that may influence dehydration tolerance (5, 6). Both quantitative and qualitative changes of proteins have been detected during dehydration stress (7). Increasing evidence indicates a relationship between the accumulation of dehydration-induced proteins and physiological adaptations to water limitation (7, 8).

Most studies on dehydration to date have mainly focused on the changes in gene expression, while there is far less information available on their functional products. The changes in gene expression are regulated by a number of different, and potentially overlapping, signal transduction pathways (9, 10). However, the level of mRNA does not always correlate well with the level of protein, the key player in the cell (11, 12). It is thus insufficient to predict protein expression level from quantitative mRNA data. Proteome studies aim at the complete set of proteins encoded by the genome and thus complement the transcriptome studies. Nevertheless, the resolution of protein spots on a two-dimensional gel is limited by several factors such as protein abundance, size, hydrophobicity, and other electrophoretic properties (13). Therefore, the complete proteome is not

---

From the National Institute for Plant Genome Research, Aruna Asaf Ali Marg, New Delhi 110067, India

Received, July 9, 2007, and in revised form, September 12, 2007
Published, MCP Papers in Press, October 6, 2007, DOI 10.1074/mcp.M700314-MCP200

© 2008 by The American Society for Biochemistry and Molecular Biology, Inc.
This paper is available on line at http://www.mcponline.org

recommended but is rather fractionated into subproteomes, to improve sensitivity and resolution and to reduce the overall complexity. Further, the compartment specific proteome is preferred because fractionated subsets of proteins provide the suitable information in which they exert their particular function (14–16). The nucleus is the subcellular organelle that contains nearly all the genetic information required for the regulated expression of cellular proteins. Nuclear proteins play key roles in the fundamental regulation of genome instability, the phases of organ development, and physiological responsiveness through gene expression. The nuclear proteome is dynamic, changing its composition in response to intracellular and environmental stimuli.

Legumes are valuable agricultural and commercial crops that serve as important nutrient sources for human diet and animal feed. The characteristic feature of legumes is the biological nitrogen fixation. Chickpea (*Cicer arietinum* L.) is one of the most important grain legumes comprising high protein content, 25.3–28.9% (17). The bulk of chickpea is produced and consumed in South Asia and increasingly in Middle East and some Mediterranean countries. India is the largest producer of chickpea in the world. It is relatively dehydration tolerant (3) and is traditionally cultivated as a second crop mostly during the dry season. Its growth is limited mainly by the content of the remaining soil moisture, and dehydration tolerance is thus the most important ecophysiological trait for determining the occurrence of reliable harvests. In a previous study, we developed the nuclear proteome map of chickpea (16). Here, we have reported the nucleus-specific comparative proteome of chickpea to identify novel components involved in dehydration tolerance with a wider aim to use them in future crop improvement program. The quantitative image analysis revealed 205 protein spots that changed their intensities significantly for more than 2.5-fold, at least, at one time point during dehydration. A total of 147 differentially expressed nuclear proteins were identified during the course of dehydration using classical two-dimensional electrophoresis coupled with LC-MS/MS. The comparison of dehydration responsive nuclear proteome in chickpea reveals predicted and unexpected components indicating their possible role in dehydration tolerance.

EXPERIMENTAL PROCEDURES

Plant Growth, Maintenance, and Dehydration Treatment—Seeds of chickpea (*Cicer arietinum* L. var. JG-62) were obtained from ICRISAT (International Crops Research Institute for the Semi-Arid Tropics), Hyderabad, India and grown in pots containing a mixture of soil and soilrite (2:1, w/w; 10 plants/1.5 L capacity pots with 18 cm diameter) in an environmentally controlled growth room. The seedlings were maintained at 25 ± 2 °C, 50 ± 5% relative humidity under 16 h photoperiod (270 μmol m^{-2} s^{-1} light intensity). The pots were provided with 100 ml of water everyday that maintained the soil moisture content to ~30%. A gradual dehydration condition was applied on the 3-week-old seedlings by withdrawing water and tissues were harvested at every 24 h up to 144 h. The unstressed and the stressed plants were kept in parallel in the same growth room. The samples from the unstressed (control) plants were collected at each time point during dehydration and were finally pooled to normalize the growth and developmental effects. The harvested unstressed and stressed tissues were instantly frozen in liquid nitrogen and stored at −80 °C.

Isolation of Pure Nuclei—The nuclei were isolated as described earlier (16). The integrity of the isolated nuclei was analyzed by staining with 4′,6′-diamidino-2-phenylindole hydrochloride (DAPI)[1]. The nuclear fraction was stained for 15 min with 0.1 μg/ml DAPI in 0.1 M potassium phosphate buffer (pH 7.4) and then washed twice with phosphate-buffered saline. For microscopy, a small volume of suspension was placed on a slide, covered with a cover glass and the images were captured with or without UV filter.

Extraction of Nuclear Protein and Two-dimensional Electrophoresis—The nuclear proteins were prepared from the nuclei-enriched pellet using TriPure Reagent (Roche) according to the manufacturer's instructions. The protein pellet was resuspended in isoelectric focusing (IEF) sample buffer [8 M urea, 2 M thiourea, and 2% (w/v) CHAPS]. The protein concentration was determined using the 2-D Quant kit (Amersham Biosciences). The enrichment of nuclear proteins was evaluated by immunoblot analysis for two nuclear resident proteins, fibrillarin and histone core. IEF was carried out with 150 μg of protein. Aliquots of proteins were diluted with two-dimensional rehydration buffer [8 M urea, 2 M thiourea, 2% (w/v) CHAPS, 20 mM dithiothreitol, 0.5% (v/v) pharmalyte (pH 4–7), and 0.05% (w/v) bromphenol blue], and 250 μl of solution was used to rehydrate immobilized pH gradient strips (13 cm; pH 4–7). Protein was loaded by in-gel rehydration method onto IEF strips, and electrofocusing was performed using the IPGphor system (Amersham Biosciences, Bucks, United Kingdom) at 20 °C for 30,000 Vh. The focused strips were subjected to reduction with 1% (w/v) dithiothreitol in 10 ml of equilibration buffer [6 M urea, 50 mM Tris-HCl (pH 8.8), 30% (v/v) glycerol and 2% (w/v) SDS], followed by alkylation with 2.5% (w/v) iodoacetamide in the same buffer. The strips were then loaded on top of 12.5% polyacrylamide gels for SDS-PAGE. The electrophoresed proteins were stained with silver stain plus kit (Bio-Rad).

Image Acquisition and Data Analysis—Gel images were digitized with a Bio-Rad FluorS equipped with a 12-bit camera. The PD Quest version 7.2.0 (Bio-Rad) was used to assemble first level matchset (master image) from three replicate two-dimensional electrophoresis gels. Experimental molecular mass and pI were calculated from digitized two-dimensional electrophoresis images using standard molecular mass marker proteins. Each spot included on the standard gel met several criteria: it was present in at least two of the three gels and was qualitatively consistent in size and shape in the replicate gels. We defined "low-quality" spots as those with a quality score <30; these spots were eliminated from further analysis. The remaining high-quality spot quantities were used to calculate the mean value for a given spot, and this value was used as the spot quantity on the standard gel. The first level matchset spot densities were normalized against the total density in the gel image. The replicate gels used for making the first level matchset had, at least, correlation coefficient value of 0.8. After obtaining the first level matchsets, a second level matchset that allowed a comparison of the standard gels from each of the time points was obtained. A second normalization was done with a set of three unaltered spots identified from across the time points. From this matchset, the filtered spot quantities from the standard gels were assembled into a data matrix of high-quality spots from the seven time points for further analysis.

---

[1] The abbreviations used are: DAPI, 4′,6′-diamidino-2-phenylindole hydrochloride; SOD, superoxide dismutase; APx, ascorbate peroxidase; NR, nitrate reductase; DRPs, dehydration responsive proteins; HDAC, histone deacetylase; GAPDH, glyceraldehyde-3-phosphate dehydrogenase; MDH, malate dehydrogenase; GRPs, glycine-rich proteins; ROS, reactive oxygen species; ABA, abscisic acid.

Protein Identification and Expression Clustering—Protein samples were excised mechanically using pipette tips, destained, in-gel digested with trypsin and peptides extracted according to standard techniques (18). Peptides were analyzed by electrospray ionization time-of-flight mass spectrometry (LC/MS/TOF) using an Ultimate 3000 HPLC system (Dionex) coupled to a Q-Trap 4000 mass spectrometer (Applied Biosystems). Tryptic peptides were loaded onto a C18PepMap100, 3 m (LC Packings) and separated with a linear gradient of water/acetonitrile/0.1% formic acid (v/v). The MS/MS data were extracted using Analyst Software v.1.4.1 (Applied Biosystems). Peptides were identified by searching the peak-list against the MSDB 20060831 (3239079 sequences; 1079594700 residues) database using the MASCOT v.2.1 (http://www.matrixsciences.com) search engine. Because the chickpea genome sequence is not known, a homology based search was performed. The database search criteria were: taxonomy, Viridiplantae (Green Plants, 247882 sequences); peptide tolerance, ±1.2 Da; fragment mass tolerance, ±0.6 Da; maximum allowed missed cleavage, 1; variable modifications, methionine oxidation; instrument type, ESI-QUAD-TOF. Protein scores were derived from ions scores as a non-probabilistic basis for ranking protein hits and the protein scores as the sum of a series of peptide scores. The score threshold to achieve $p < 0.05$ is set by Mascot algorithm and is based on the size of the database used in the search. The details regarding the precursor ion mass, expected molecular weight, theoretical molecular weight, delta, score, rank, charge, number of missed cleavages, p value, and the peptide sequence for proteins identified with a single peptide are mentioned in supplemental document 1. Further, the fragment spectra for these proteins are provided in supplemental document 2. Wherein there were more than one accession numbers for the same peptide, the match was considered in terms of putative function. In the case of same protein being identified in multiple spots where several peptides were found to be shared by the isoforms, differential expression pattern was observed for each of the candidate and thus the proteins were listed as independent entities. The function of each of the identified protein has been analyzed in view of the metabolic role of the candidate protein in the nucleus. The protein functions were assigned using a protein function database Pfam or Inter-Pro. As functional annotation is based on pFam and Interpro, the functional redundancy, if any, is thus greatly minimized.

Self-organizing tree algorithm (SOTA) clustering was performed on the log transformed fold induction expression values across seven time points by using Multi Experiment Viewer software (TIGR). The clustering was done with Pearson correlation as distance with 10 cycles and maximum cell diversity of 0.8 (19).

Immunoblot Analysis—Immunoblotting was done by resolving nuclear protein on a uniform 12.5% SDS-PAGE and then electrotransferring onto nitrocellulose membrane at 150 mA for 2 h. The membranes were subsequently blocked with 5% (w/v) nonfat milk for 1 h and incubated with respective primary antibodies for 2 h. Further, the blots were incubated with alkaline phosphatase conjugated secondary antibody for 1 h and the signal was detected using nitro blue tetrazolium/5-bromo-4-chloro-3-indolyl phosphate method.

Enzyme Assays—The isolated nuclei pellet was suspended and homogenized in 100 mM triethanolamine (Tea, pH 7.4) for superoxide dismutase (SOD), 50 mM of KPO_4^- buffer (pH 7.0) for ascorbate peroxidase (APx), and 57 mM KPO_4^- buffer (pH 7.5) for nitrate reductase (NR), respectively. The homogenate was centrifuged at 16,000 × *g* for 20 min at 4° C. The supernatant was transferred into fresh tube and was used for the assay of SOD, APx, and NR.

SOD activity was determined by spectrophotometric method based on the inhibition of superoxide-driven NADH oxidation (20). The assay mixture contained 100 mM triethanolamine (pH 7.4), 100 mM/50 mM EDTA/$MnCl_2$, 7.5 mM NADH, and 10 mM mercaptoethanol in a total volume of 1.0 ml. The oxidation of NADH was followed at 340 nm (an absorbance coefficient of 6.2 mM^{-1} cm^{-1}). The oxidation rates were initially low, then increased progressively (usually 2–4 min after mercaptoethanol addition) to yield a linear kinetics (12–15 min), which were used for calculation. APx was assayed from the decrease in absorbance at 290 nm (an absorbance coefficient of 2.8 mM^{-1} cm^{-1}) as ascorbate is oxidized by its activity (21). The reaction mixture for the peroxidase contained 50 mM potassium phosphate (pH 7.0), 0.5 mM ascorbate, and 0.1 mM H_2O_2 in a total volume of 1.0 ml. The reaction was initiated by adding H_2O_2, and the absorbance was recorded 30 s after the addition. Correction was done for the low, nonenzymatic oxidation of ascorbate by H_2O_2. On the other hand, the activity of NR was determined in the reaction mixture containing 57 mM potassium phosphate (pH 7.5), 0.005 mM FAD, 0.2 mM NADPH, and 10 mM potassium nitrate. The oxidation of NADH was followed at 340 nm (an absorbance coefficient of 6.2 mM^{-1} cm^{-1}) for ~5 min and the maximum linear rate was used to calculate the activity (22).

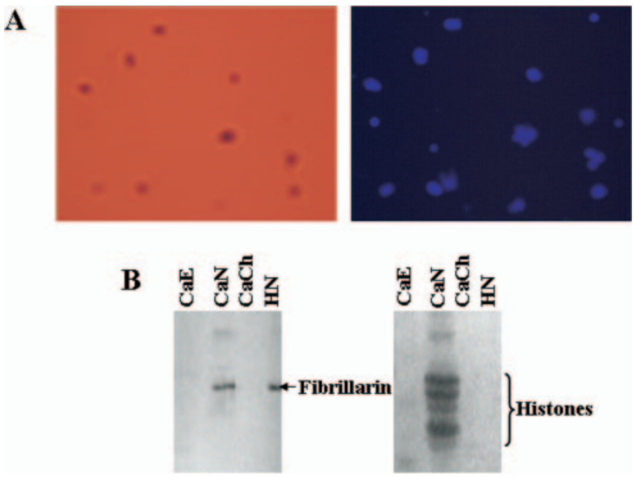

FIG. 1. **Analysis of isolated chickpea nuclear fraction.** *A*, the purified nuclear fraction was stained with DAPI and visualized by confocal microscopy. Phase contrast micrograph of the nuclei is shown in the *left panel*, while the DAPI-stained nuclei are shown in the *right panel*. *B*, immunoblot analysis of extracted nuclear proteins with anti-histone core and anti-fibrillarin antibodies. Aliquots of 100 μg of protein, each from nuclear (*CaN*), chloroplast (*CaCh*), and ECM (*CaE*) fractions of chickpea, as well as HeLa nuclear extract (*HN*), were separated by 12.5% SDS-PAGE. HeLa nuclear extract was used as positive control, whereas chloroplast and ECM fractions were used as negative controls. The one-dimensional gel was electroblotted onto Hybond-C membrane, and histones and fibrillarin were detected using alkaline phosphatase conjugated secondary antibodies.

RESULTS

Two-dimensional Electrophoresis of Nuclear Proteins of Chickpea—The primary objective of this study was to characterize global protein expression in nucleus of chickpea during dehydration. Chickpea seedlings were subjected to gradual dehydration over 144 h. There were no visible changes in the seedlings during 24 h of dehydration. The leaflets rolled after 36 h of dehydration, and the damage aggravated further during 48–144 h. The nuclei were isolated from the seedlings using hyperosmotic sucrose buffer, and the nuclei enriched pellet so obtained was washed repeatedly to get rid of contaminants from other organelles. The integrity of the isolated nuclei was analyzed by DAPI staining (Fig. 1*A*). The nuclear

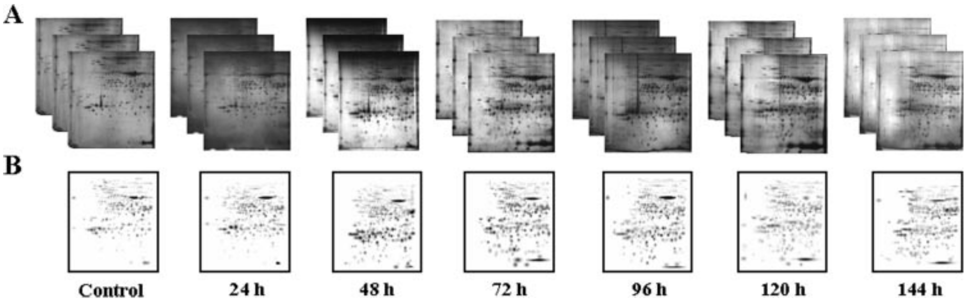

FIG. 2. **Dehydration responsive comparative proteome of chickpea nucleus and the representative two-dimensional gel electrophoresis.** Three-week-old chickpea seedlings were subjected to dehydration and tissue harvested every 24 h until 144 h. The nuclear proteins were isolated from the control and the stressed tissue. An equal amount (150 μg) of protein from each time point was separated by two-dimensional gel electrophoresis. Three replicate gels for each time point (*A*) were computationally combined using PDQuest software to generate the standard gels (*B*).

proteins were prepared from the purified nuclei using TriPure reagent (Roche Diagnostics) to remove the contaminating nucleic acids, which might interfere during the IEF process. The enrichment of nuclear proteins was evaluated by immunoblot analysis using specific antibodies for two nuclear proteins, fibrillarin and histone core (Fig. 1*B*). Isolated nuclear proteins from control and dehydrated chickpea seedlings were resolved and detected using high-resolution two-dimensional electrophoresis followed by silver staining as detailed in "Experimental Procedures." For each time point, three replicate two-dimensional electrophoresis gels were run, which were then computationally combined into a representative standard gel (Fig. 2). The only spots that survived several stringent criteria (classified as "high-quality" spots) were used to estimate spot quantities; otherwise, a large number of protein spots were included in the matchset. For example, 321 spots were detected in the control gel, but 316 were classified as high quality (Table I). The spot densities at the lower level were normalized against the total density present in the respective gel to overcome the experimental errors introduced due to differential staining. To make comparison between the time points, a second level matchset was created (Fig. 3). The intensity of spots was normalized to that of landmark proteins used for internal standardization. From the higher level matchset, the filtered spot quantities were assembled into a data matrix that consisted of 501 unique spots indicating change in intensity for each spot during dehydration. The data reveal that nearly 95% of the spots on the standard gels were of high quality reflecting the reproducibility of the experimental replicates (Table I).

More than 400 protein spots were reproducibly detected on silver-stained gels. Quantitative image analysis revealed a total of 205 protein spots that changed their intensities significantly by more than 2.5-fold at least at one time point. While most spots showed quantitative changes, some spots showed qualitative changes also. Six typical gel regions are enlarged as shown in Fig. 4. Of the 205 dehydration responsive proteins (DRPs), 80 proteins were clearly up-regulated and 46 were down-regulated, while 79 proteins showed a mixed pattern of time-dependent expression.

TABLE I
Reproducibility of 2-dimensional gels

Time	Average no. of spots[a]	High quality spots[b]	Reproducibility
Control (*h*)	321	316	98.44%
24	310	287	92.58
48	344	330	95.93
72	305	279	91.48
96	312	298	95.51
120	258	248	96.12
144	299	291	97.65
Total	2149	2049	95.34

[a] Average number of spots present in three replicate gels of each time point.

[b] Spots having quality score more than 30 assigned by PDQuest (Ver.7.2.0).

Identification of the Differentially Expressed Proteins—MS/MS analysis was carried out for 147 DRPs resulting in 105 proteins with a significant match, representing an identification success rate of ~70%. As an advantage of using classical two-dimensional electrophoresis, we could detect different isoelectric species of various proteins. For example, five isoelectric species were detected for glyceraldehyde-3-phosphate dehydrogenase (GAPDH), which is suggestive of post-translational modification(s). This type of information cannot be acquired using transcriptomic approaches. Although adept at resolving isoelectric species, the technique of two-dimensional electrophoresis is somewhat restricted at quantifying low abundance proteins. This might account for the absence of many of the transcription factors in differential proteome of chickpea nucleus. Despite the known limitation of current two-dimensional electrophoresis methodology at detecting underrepresented proteins, the differential expression pattern of 105 nuclear proteins would nevertheless help in elucidating the complex regulatory network involved in dehydration tolerance.

The identified DRPs might play a variety of functions during cellular adaptation against dehydration, *e.g.* gene regulation,

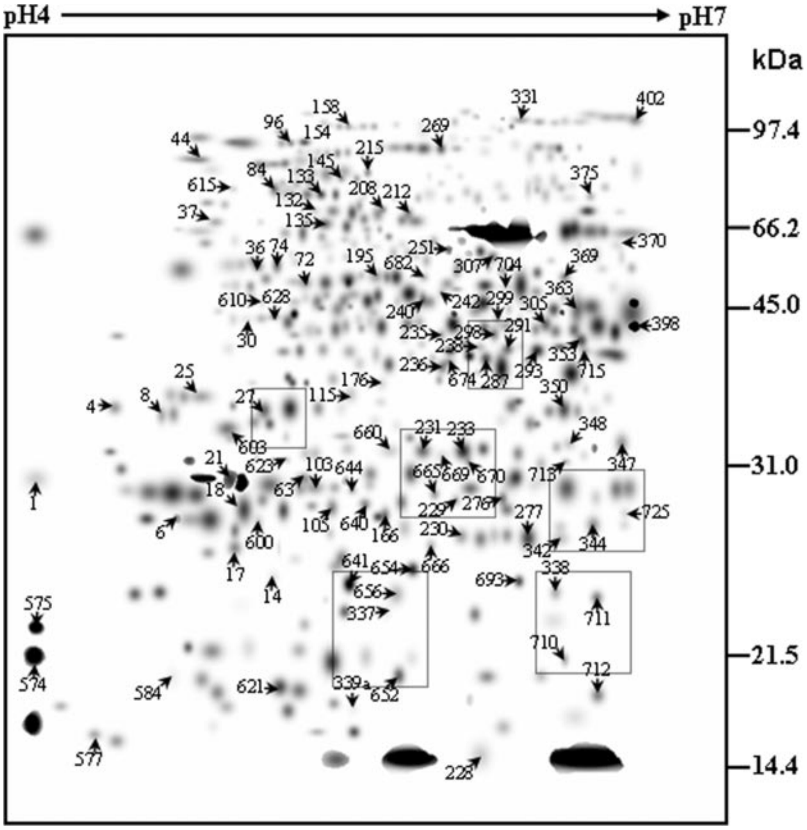
pH4
pH7
kDa
97.4
66.2
45.0
31.0
21.5
14.4
158
331
402
96
154
269
44
215
145
84
133
375
615
132
208
212
37
135
370
36
74
72
195
251
682
307
704
369
363
610
628
240
242
299
305
398
235
298
291
30
238
353
236
25
176
674
287
293
715
350
8
4
27
115
660
231
233
348
603
21
623
103
644
665
669
670
713
347
18
63
229
276
725
1
6
105
640
166
230
277
600
342
344
17
641
654
666
693
338
14
656
575
337
711
710
574
584
621
339
652
712
577
228

FIG. 3. **Higher level matchset of protein spots detected by two-dimensional gel electrophoresis.** The matchset was created *in silico* from seven standard gels for each of the time point as depicted in Fig. 2. The *boxed areas* marked with *dotted lines* represent the zoomed in gel sections in Fig. 4. The numbers correspond with the spot ID mentioned in Table II.

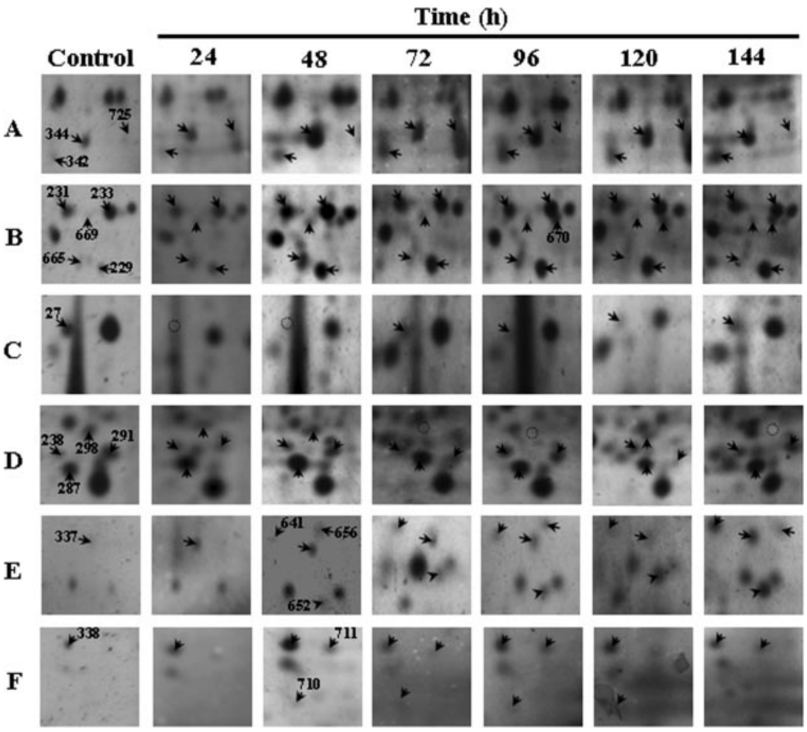
Time (h)
Control
24
48
72
96
120
144
A
B
C
D
E
F
344
725
342
231
233
669
665
229
670
27
238
298
291
287
337
641
656
652
338
711
710

FIG. 4. **Time-dependent changes of the differentially expressed proteins.** Boxed areas (*A-F*) are zoomed in gel sections and correspond to the *boxed areas* in Fig. 3.

signaling, proteolysis, and chaperone type activities. All the identified DRPs were grouped into 10 functional classes based on their respective roles in dehydration response (Fig. 5 and Table II). The proteins for which no known function could be assigned were grouped under the unknown category that accounted for 24% of the dehydration responsive nuclear

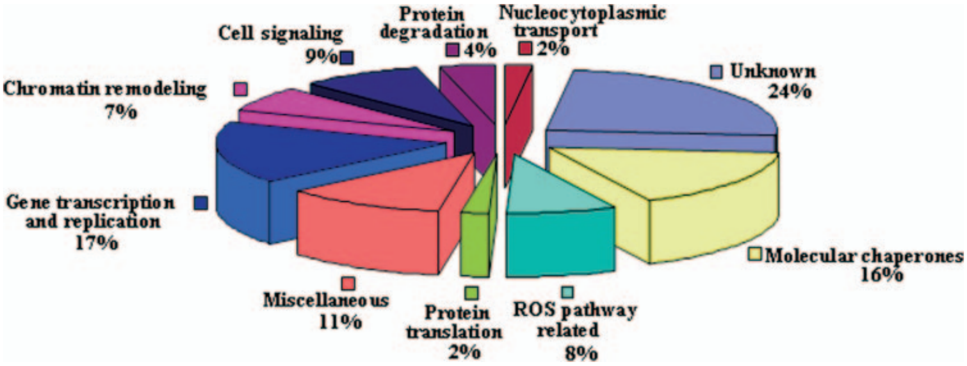

FIG. 5. **Functional cataloging of DRPs in chickpea nucleus.** The identified DRPs were assigned a putative function using Pfam and Interpro databases and functionally categorized as represented in the pie chart.

proteome. Gene transcription and replication (17%) were found to be the most abundant class of proteins, reflecting the role of nucleus in gene expression and regulation. This was closely followed by the molecular chaperones (16%), which might help in protecting and proper functioning of the cellular machinery following dehydration stress. The cell signaling, chromatin remodeling, protein degradation, and the reactive oxygen species (ROS) pathway related proteins were other major classes identified. Some of these DRPs are likely to be breakdown products as is evident from the gel-based size of these proteins and have been discussed in that light.

Dynamics of Protein Networks during Dehydration—To summarize the information contained in Table II and to cluster the proteins showing similar expression profiles during dehydration response in chickpea, self-organizing tree algorithm clustering was applied to the DRPs. The data were taken in terms of fold expression with respect to the control expression value. Further, the data sets were log transformed to the base two in order to level the scale of expression and to reduce the noise. The analysis yielded 11 expression clusters and only the clusters with $n \geq 10$ were taken to study the coexpression patterns for functionally similar proteins (Fig. 6). Detailed information on proteins within each cluster can be found in supplemental Fig. 1.

Cluster 1 and 2 both were found to be early dehydration responsive; however, no clear clustering pattern was detected for either of them. Almost all the functional categories are represented in these two clusters. The proteins in Cluster 5 first decreased in relative expression followed by a gradual increase during late dehydration. This cluster is enriched in the ROS pathway-related proteins. Cluster 6, with 17 members, showed maximum co-clustering for the proteins involved in gene transcription and replication. Nonhomogeneous expression patterns were observed for different subunits in protein complexes. For example, dnaK and dnaJ were present in Clusters 5 and 4, respectively, which might underline the complexity of such responses. The unknown category of proteins comprised a major fraction in all the clusters. The fact that the unknown proteins were identified as dehydration responsive gives the first functional annotation to these genes. Identification of these proteins can provide valuable insight into the kinetics of dehydration tolerance mechanisms.

Immunoblot Analysis—Several proteins were identified as the same protein having the same molecular weight but different pI values that were expressed differentially during dehydration, including GAPDH and malate dehydrogenase (MDH). Previously, we showed that some other isoforms of the same protein are also a part of the chickpea nuclear proteome (16) even though these were not found to be differentially expressed under dehydration. Changes in protein levels alone do not imply changes in function as many proteins are known to be regulated by post-translational modifications. Proteins can resolve into multiple spots due to proteolytic processing, multiple isoforms, or changes in charge state resulting from posttranslational modifications, including phosphorylation, deamidation, acetylation, glycation, and glutathionylation (23–26). It is possible that post-translational modifications may affect in-gel migration of a protein such that a protein classified as repressed may be present elsewhere on the gel or that a putative *de novo* protein may be found in a new place in the gel. Because some proteins migrated in multiple spots, we have used one-dimensional Western blot analysis to determine whether changes in individual isoelectric variants were representative of the entire protein population. GAPDH and MDH along with 14-3-3 and dnaK were subjected to immunoblot analysis in an attempt to address this discrepancy. 14-3-3 and dnaK both followed exactly the same profile as detected on the two-dimensional electrophoresis gel (Fig. 7 and Table II). GAPDH, which was represented by nine spots (5 differentially expressed and 4 with constitutive expression) on the two-dimensional electrophoresis gel, showed two bands on the one-dimensional Western blot, each showing a different profile. MDH, which had three spots (1 differentially expressed and 2 with constitutive expression) on the two-dimensional electrophoresis gel, showed an up-regulation toward the later time points (Fig. 7).

Effect of Dehydration on SOD, APx, and NR—The functional

TABLE II

List of dehydration responsive chickpea nuclear proteins identified by MS/MS analysis

Functional category	Spot ID[a]	Score	Identification	gi no.[b]	No. of peptides	Protein expression profile[c] C 24 48 72 96 120 144	% Coverage	Thr MW/pI	Exp MW/pI
Cell signaling	CaN-1	50	FCA protein (fragment)	32482057	1	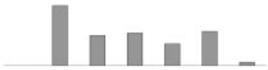	5%	29.37/8.63	31.00/4.00
	CaN-236	46	FCA protein (Fragment)	32482140	1	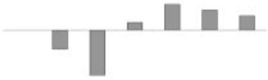	2%	79.49/8.85	41.32/5.89
	CaN-711	43	FCA protein (Fragment)	32482057	2	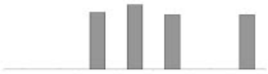	5%	29.37/8.63	21.93/6.65
	CaN-8	173	14-3-3-like protein	4775555	4	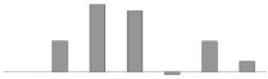	13%	29.42/4.71	36.76/4.60
	CaN-229	45	Protein kinase 2	7573598	1	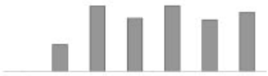	1%	45.30/7.11	29.86/6.00
	CaN-305	42	Serine-threonine kinase	38194927	2	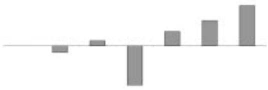	5%	45.58/5.48	46.78/6.39
	CaN-623	35	Hypothetical protein OSJNBa0011L09.21 (Protein-tyrosine-phosphatase, putative)	20503032	1	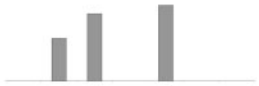	2%	40.63/6.21	32.87/5.22
	CaN-640	54	Hybrid type histidine kinase	82466315	3	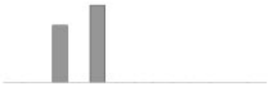	2%	113.17/8.65	29.70/5.50
	CaN-693	40	Similarity to receptor-like protein kinase	9758282	2	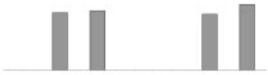	4%	71.94/9.44	23.10/6.26
Gene transcription and replication	CaN-4	41	Aspartate carbamoyltransferase	15796550	1	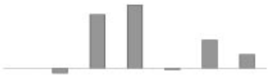	2%	42.57/6.06	37.37/4.35
	CaN-276	48	Aspartate carbamoyltransferase	15796550	2	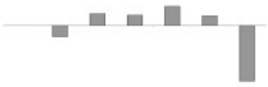	3%	42.57/6.06	29.95/6.22
	CaN-287	40	Aspartate carbamoyltransferase	15796550	2	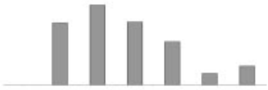	3%	42.57/6.06	42.20/6.15
	CaN-242	226	Glyceraldehyde-3-phosphate dehydrogenase B subunit	77540212	5	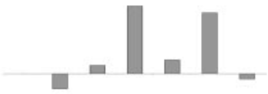	11%	48.20/7.10	52.63/5.92
	CaN-269	548	glyceraldehyde-3-phosphate dehydrogenase (phosphorylating)	309671	11	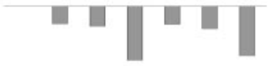	24%	48.06/7.57	98.51/5.91
	CaN-363	211	glyceraldehyde-3-phosphate dehydrogenase (phosphorylating)	12159	4		10%	43.31/8.80	49.49/6.60

TABLE II—*continued*

						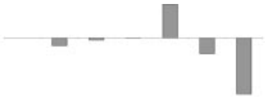			
	CaN-398	303	glyceraldehyde-3-phosphate dehydrogenase (phosphorylating)	12159	6	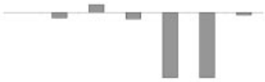	14%	43.31/ 8.80	46.39 /6.85
	CaN-682	417	Glyceraldehyde-3-phosphate dehydrogenase, type I	92875110	10	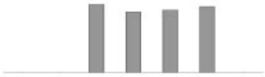	17%	47.91/ 6.76	56.07 /5.83
	CaN-251	255	Transketolase (Fragment)	4586600	5	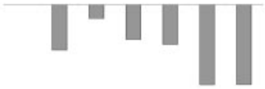	32%	17.12/ 5.84	64.47 /5.97
	CaN-299	199	Fructose-bisphosphate aldolase (EC 4.1.2.13)	40457267	3	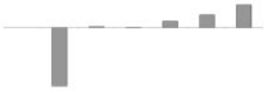	9%	38.37/ 6.77	47.49 /6.16
	CaN-628	60	OSJNBa0042F21.13 protein- Fructose-1,6-bisphosphatase	38347311	3	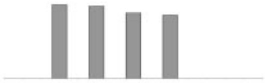	5%	42.22/ 5.64	47.99 /5.16
	CaN-18	36	Putative transcription factor	12328532	2	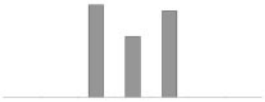	1%	64.97/ 6.55	28.65 /5.02
	CaN-36	66	AAA ATPase, central region; Homeodomain-like	92874675	2	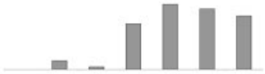	3%	52.13/ 5.42	59.75 /5.10
	CaN-208	43	Retrotransposon protein, putative, Ty1-copia subclass	77555208	2	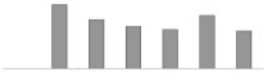	2%	91.96/ 9.33	76.28 /5.62
	CaN-233	37	Homeobox-leucine zipper protein, putative	89257493	1	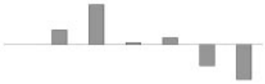	3%	30.88/ 8.50	33.59 /6.02
	CaN-331	41	AP2/EREBP transcription factor BABY BOOM	58761187	2	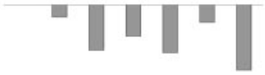	2%	64.50/ 5.99	76.22 /6.22
	CaN-338	37	AY045676 NID (WRKY-DNA binding domain)	27363252	2	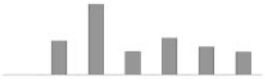	3%	55.78/ 8.18	22.30 /6.42
	CaN-713	35	Homeobox protein HB3 (Fragment)	46408855	2	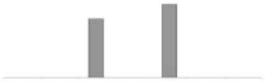	5%	27.06/ 11.83	32.71 /6.48
Chromatin remodeling	CaN-72	110	Actin	58533119	3	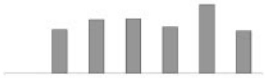	8%	41.70/ 5.23	55.61 /5.27
	CaN-103	56	Kinesin-related protein	14041829	3	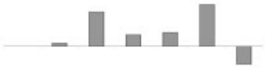	1%	118.68 /8.14	30.76 /5.30
	CaN-230	47	Putative MAR binding filament-like protein 1	55296302	1	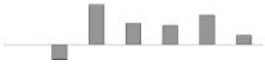	1%	84.08/ 5.00	27.51 /6.02

TABLE II—*continued*

	CaN-574	42	Histone H3, putative, expressed	77555106	2	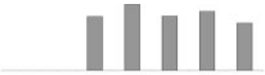	14%	15.42/11.06	18.40/4.03
	CaN-575	74	At5g59910- histone H2B	16323079	3	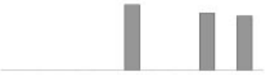	16%	16.44/10.00	20.09/4.05
	CaN-240	31	DNA cytosine methyltransferase Zmet3, putative	77553397	1	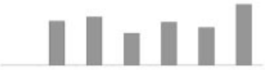	1%	49.60/5.25	51.38/5.83
	CaN-603	50	Histone deacetylase HDA110	22135469	1	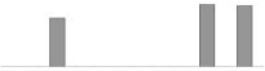	2%	43.45/8.63	34.63/4.96
ROS pathway related	CaN-6	62	2-cys peroxiredoxin-like protein (Fragment)	47027073	1	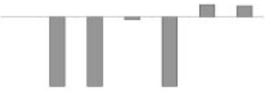	7%	21.84/4.93	27.90/4.71
	CaN-158	41	NADPH oxidase	87116554	2	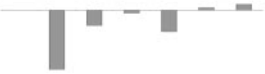	2%	105.19/9.12	105.77/5.49
	CaN-176	62	Glyoxalase/bleomycin resistance protein/dioxygenase	92887944	2	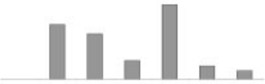	6%	32.22/5.13	39.69/5.64
	CaN-231	123	L-ascorbate peroxidase	71534930	2	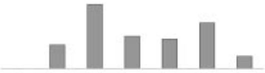	16%	13.16/9.44	33.63/5.80
	CaN-293	247	Malate dehydrogenase (EC 1.1.1.37)	10334493	5	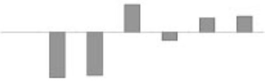	17%	35.47/5.92	43.05/6.37
	CaN-344	180	superoxide dismutase (EC 1.15.1.1) (Mn) 1 [similarity]	6006619	4	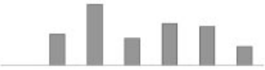	12%	25.44/8.62	27.33/6.63
	CaN-615	36	Putative O-acetylserine (Thiol)-lyase	56785056	3	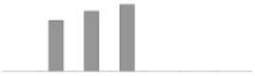	4%	41.27/5.53	82.03/4.97
	CaN-644	60	MCR250951 NID-glutathione peroxidase	18073933	2	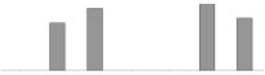	13%	18.91/6.59	30.35/5.51
Molecular chaperones	CaN-25	46	Putative glycine-rich RNA-binding protein 2	6911146	1	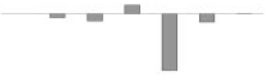	9%	16.25/7.82	38.39/4.72
	CaN-63	48	Putative glycine-rich RNA binding protein 1	6911146	1	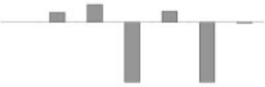	9%	16.25/7.82	31.41/5.25
	CaN-132	52	Putative glycine-rich RNA-binding protein 2	6911146	1	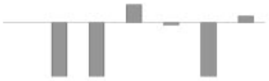	9%	16.25/7.82	74.02/5.34
	CaN-166	62	Putative glycine-rich RNA-binding protein 2	6911146	2	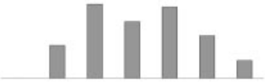	15%	16.25/7.82	28.85/5.64
	CaN-277	79	Putative glycine-rich RNA-binding protein 2	6911146	3		22%	16.25/7.82	27.41/6.33

TABLE II—*continued*

						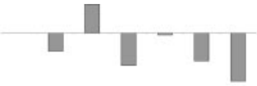			
	CaN-339	61	Putative glycine-rich RNA binding protein 2	6911144	1	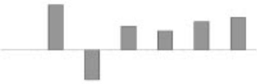	8%	16.25/ 7.82	15.00 /6.60
	CaN-375	45	Putative glycine-rich RNA-binding protein 2	6911146	1	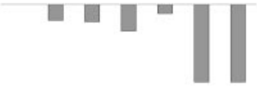	9%	16.25/ 7.82	80.40 /6.64
	CaN-577	41	Putative glycine-rich RNA-binding protein 2	6911146	1	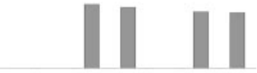	9%	16.25/ 7.82	14.49 /4.33
	CaN-44	433	dnaK-type molecular chaperone CSS1 precursor	169023	9	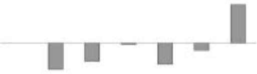	13%	75.47/ 5.22	93.45 /4.77
	CaN-715	45	Heat shock protein DnaJ, N-terminal	92896166	2	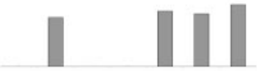	7%	53.40/ 7.12	42.96 /6.58
	CaN-600	45	dehydrin homolog Wcs66	440847	1	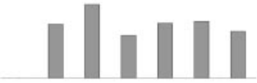	1%	46.77/ 6.74	27.45 /5.09
	CaN-641	249	heat shock protein 18.2	19618	6	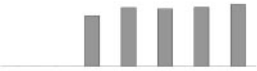	27%	18.15/ 5.84	22.87 /5.50
	CaN-654	73	Heat shock protein Hsp20	87240494	3	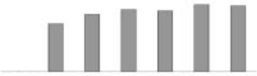	16%	18.18/ 5.81	23.90 /5.79
	CaN-17	106	Beta-conglutin	46451223	2	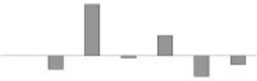	5%	62.09/ 6.43	26.75 /4.90
	CaN-656	68	vicilin B precursor	137581	1	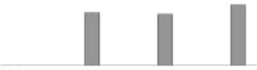	2%	46.36/ 5.39	22.19 /5.71
	CaN-133	276	probable chaperonin 60 beta chain	806808	6	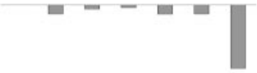	10%	62.94/ 5.85	81.15 /5.36
	CaN-584	46	Maturase K (Fragment)	38532287	3	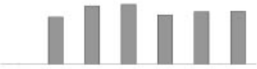	7%	40.42/ 10.13	16.75 /4.60
Protein translation	CaN-195	345	translation elongation factor EF-Tu precursor, chloroplast	20070084	8	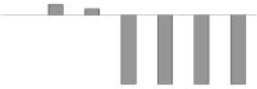	16%	53.02/ 6.62	56.22 /5.62
	CaN-610	218	translation elongation factor EF-Tu precursor, chloroplast	20070084	3	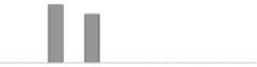	9%	53.02/ 6.62	50.62 /5.10
Protein degradation	CaN-84	440	Putative FtsH-like protein Pftf	52075838	8	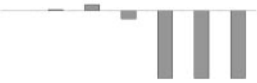	11%	72.49/ 5.54	83.12 /5.19
	CaN-342	37	Cyclin-like F-box; Agenet	92879072	1		2%	59.22/ 7.84	26.23 /6.45

Table II— *continued*

						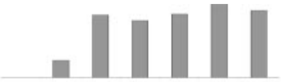			
	CaN-350	41	Hypothetical protein (kelch repeat-containing F-box family protein)	48210029	2	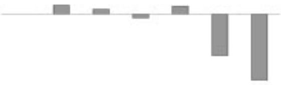	4%	56.81/ 4.93	37.23 /6.47
	CaN-370	74	AF041258 NID (ATP-dependent 26S proteasome regulatory subunit)	3914449	1	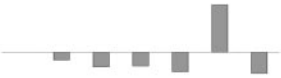	2%	47.52/ 6.43	62.94 /6.70
Nucleocytoplasmic transport	CaN-212	44	Hypothetical protein At1g55040-zf-RanBP	15293147	1	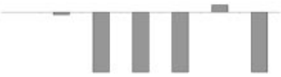	1%	94.74/ 6.72	75.11 /5.72
	CaN-347	131	ATRRAN2	1668706	4	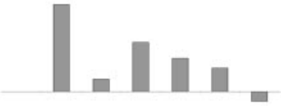	19%	25.02/ 6.65	34.24 /6.79
Miscellaneous	CaN-105	47	AtpB (Fragment)	6110504	3	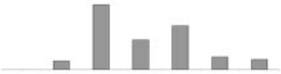	88%	10.72/ 12.00	29.33 /5.38
	CaN-235	40	ATPase beta subunit	3676294	1	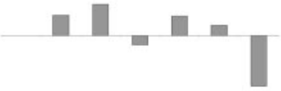	1%	59.87/ 5.83	44.71 /5.91
	CaN-135	366	H+-transporting two-sector ATPase (EC 3.6.3.14) beta chain	18831	5	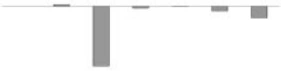	9%	60.22/ 5.95	69.46 /5.39
	CaN-298	85	H+-transporting two-sector ATPase (EC 3.6.3.14) gamma chain precursor	19785	1	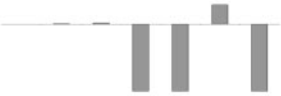	3%	41.42/ 8.16	55.03 /6.15
	CaN-353	101	H+-transporting two-sector ATPase (EC 3.6.3.14) gamma chain precursor	19785	2	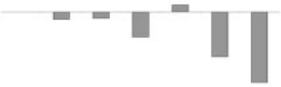	7%	41.42/ 8.16	44.10 /6.60
	CaN-660	43	H(+)-transporting ATP synthase (EC 3.6.1.34) (Fragment)	4995757	2	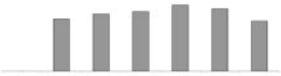	5%	52.45/ 5.15	33.81 /5.64
	CaN-402	153	glycine dehydrogenase (decarboxylating) component P precursor	20741	4	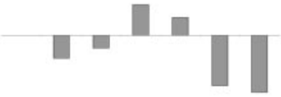	3%	114.61 /7.17	108.0 /6.85
	CaN-291	54	2'-hydroxy isoflavone reductase-transcriptional repressor activity	17949	3	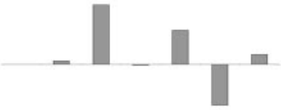	9%	35.38/ 5.94	43.26 /6.23
	CaN-369	65	F18O14.30 (similar to isoflavone reductase)	8778426	1	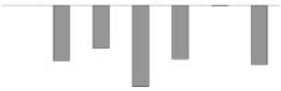	3%	35.37/ 5.58	56.92 /6.52

TABLE II—*continued*

	CaN-674	100	Phenylcoumaran benzylic ether reductase-like protein Fi1	90811671	2	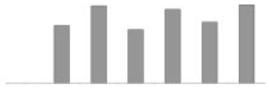	5%	34.35/ 5.44	41.90 /5.95
	CaN-710	46	Nitrate reductase (EC 1.6.6.1) (EC 1.6.6.2) (EC 1.6.6.3)	6573214	2	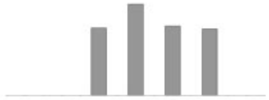	1%	97.71/ 5.92	18.20 /6.48
	CaN-238	37	NBS-LRR type disease resistance protein Rps1-k-1	62632823	2	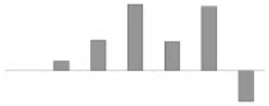	1%	139.71 /7.29	43.42 /6.09
Unknown	CaN-14	45	Hypothetical protein At4g02550/T10P11_16	26449957	1	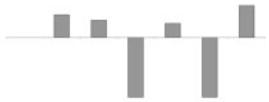	3%	32.36/ 8.76	23.33 /5.16
	CaN-21	46	Hypothetical protein OSJNBb0011H15.25	42408955	1	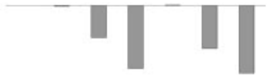	10%	16.54/ 10.47	31.20 /4.87
	CaN-27	46	Brain protein 44-like	37806192	1	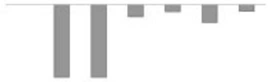	7%	12.07/ 8.71	37.15 /5.09
	CaN-30	40	Putative polyprotein	23266291	1	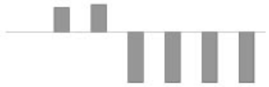	2%	71.19/ 7.55	47.36 /5.03
	CaN-37	47	OSJNBa0011F23.7 protein	38346401	1	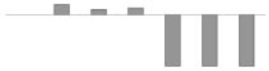	1%	49.05/ 6.00	72.05 /4.80
	CaN-74	119	At2g39730/T5I7.3	23308421	2	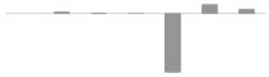	3%	51.97/ 5.69	59.96 /5.18
	CaN-96	58	Hypothetical protein At1g62750	14532624	2	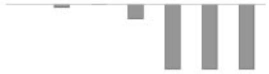	2%	85.94/ 5.48	97.0/ 5.21
	CaN-115	45	Protein At4g02550	7269015	1	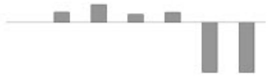	3%	37.65/ 8.72	38.61 /5.50
	CaN-145	41	Hypothetical protein P0031A09.11	53792900	2	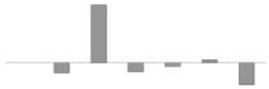	12%	15.91/ 9.61	86.61 /5.48
	CaN-154	45	Hypothetical protein P0033D06.7	52353656	2	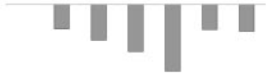	2%	64.81/ 7.57	94.75 /5.40
	CaN-215	43	Hypothetical protein At2g43170	51970954	1	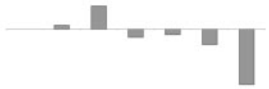	1%	95.42/ 5.63	88.90 /5.59
	CaN-228	43	Brain protein 44-like	37806192	1	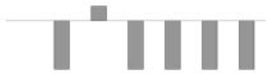	7%	12.07/ 8.71	15.00 /6.10
	CaN-307	41	OSJNBa0049H08.9 protein	38347658	2		2%	93.70/ 5.87	62.09 /6.18

TABLE II—*continued*

					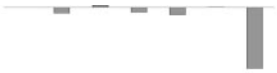			
CaN-337	41	hypothetical protein F7A19.27	5080794	2	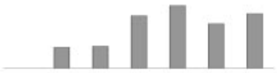	4%	55.38/8.31	21.07/5.66
CaN-339a	44	Hypothetical protein (Fragment)	86438763	1	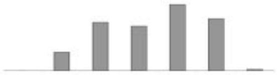	3%	26.50/5.51	15.67/5.52
CaN-348	42	protein F21J9.20 [imported]	9743340	2	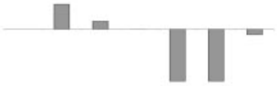	4%	61.01/9.10	34.25/6.50
CaN-621	158	Putative ABA-responsive protein	6469115	5	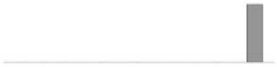	48%	16.66/5.17	16.74/5.18
CaN-652	39	Hypothetical protein OSJNBb0035I14.1	54290266	2	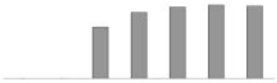	3%	23.07/11.70	17.33/5.72
CaN-665	46	hypothetical protein At2g23880 [imported]	75220227	2	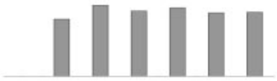	1%	139.43/9.46	30.02/5.88
CaN-666	41	OSJNBb0004A17.14 protein	70663950	1	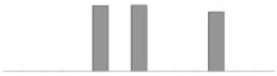	2%	44.38/6.11	25.61/5.87
CaN-669	44	AC027036 NID	14475950	2	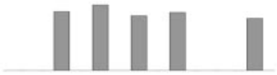	1%	132.93/7.13	31.64/5.87
CaN-670	49	Hypothetical protein P0229B10.2	50726594	1	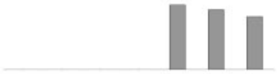	1%	53.42/5.61	32.64/6.04
CaN-677a	44	OSJNBa0089N06.25 protein	21741073	2	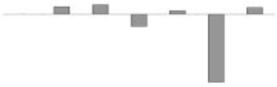	3%	16.21/11.70	49.00/6.07
CaN-704	44	OSJNBb0004A17.14 protein	70663950	1	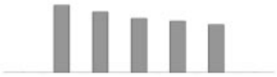	2%	44.38/6.11	53.82/6.21
CaN-712	46	Hypothetical protein P0445H04.14	55773857	1	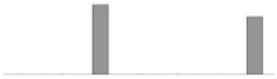	3%	29.99/11.95	16.34/6.65
CaN-725	47	hypothetical protein At2g38370 [imported]	3395435	3	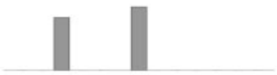	3%	60.29/9.07	28.33/6.81

---

[a] Spot number as given on the two-dimensional gel images. The first letters (Ca) signify the source plant, *Cicer arietinum,* followed by the subcellular fraction, nuclear (N). The numerals indicate the spot numbers corresponding to Fig. 3.

[b] Gene identification number as in GenBank.

[c] Protein expression profile represents the average change in spot density at various time points C (Control), 24 h, 48 h, 72 h, 96 h, 120 h and 144 h. The data were taken in terms of fold expression with respect to the control value and were log transformed to the base two in order to level the scale of expression and to reduce the noise.

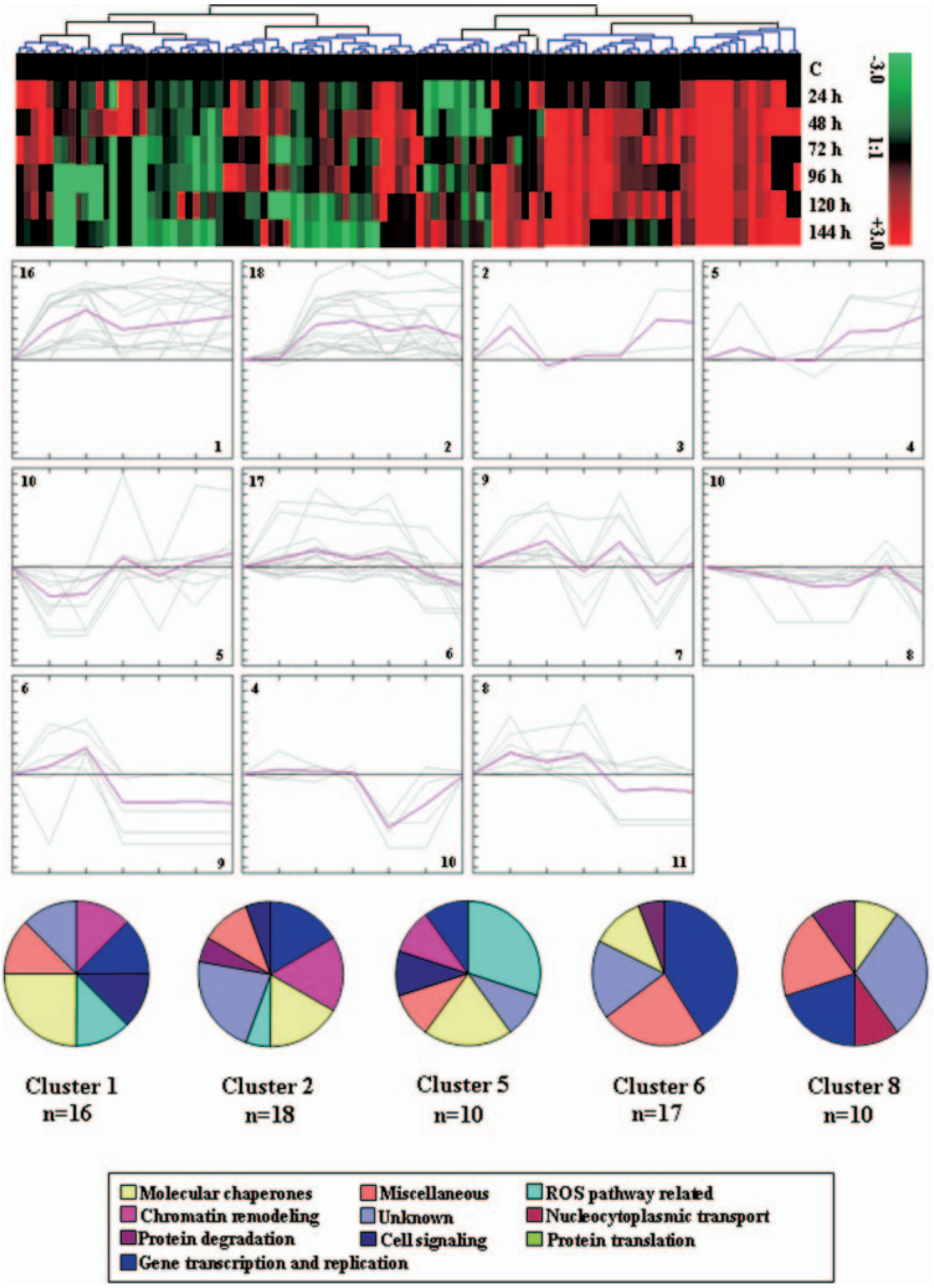

FIG. 6. **Clustering analysis of expression profiles of nucleus-specific DRPs in chickpea.** The differentially expressed 105 proteins were grouped into 11 clusters based on their expression profiles. The self-organizing tree algorithm cluster tree is shown at the *top* and the expression profile in self-organizing tree algorithm clusters are shown below. The expression profile of each individual protein in the cluster is depicted by *gray* lines, whereas the mean expression profile is marked in *pink* for each cluster. The number of proteins in each cluster is given in *left upper corner* and the cluster number in the *right lower corner*. Detailed information on proteins within each cluster can be found in supplemental Fig. 1.

aspect of an enzymatic protein is dependent on its activity rather than on its presence in the proteome. Post-translational modifications are known to affect the activity and also the fact that few of the proteins were expected to be degraded forms owing to their low molecular weight, compelled us to study the enzyme activity for few of the proteins. It is likely that dehydration stress may give rise to increased ROS levels, particularly superoxide radical (O_2^-) and hydrogen peroxide (H_2O_2) (27, 28). The SOD catalyzes the dismutation of O_2^- to molecular oxygen and H_2O_2, thus playing a key role in cell defense and rescue mechanism (29). Subsequently, H_2O_2 can be decomposed by catalase or through a series of oxidoreduction reactions involving ascorbate peroxidase (APx) and glutathione peroxidase (GPx) using ascorbate or reduced glutathione, respectively. Because oxidative stress pathway appeared to play a very important role in the dehydration responsive chickpea nuclear proteome, we investigated the behavior of the antioxidant enzymes, SOD and APx, under dehydration. The enzyme assay showed that both SOD and APx had maximum activity during early stress perception (48 h), whereas APx also showed a late induction at 120 h of dehydration stress. Furthermore, SOD displayed ~3-fold increase in activity, whereas APx showed a maximum increase of less than 2-fold (Fig. 8).

Dehydration is known to cause increased NR protein turnover (30). NR was identified as a degraded product with a lower molecular weight than expected (Table II). The activity graph of NR showed that the activity goes down until 72 h and then tries to recover a little (Fig. 8), which indicates that NR is also present as an intact protein in the chickpea nuclear proteome. However, under dehydration stress, the NR protein might undergo degradation even though a direct relationship between the accumulation of degraded product and the activity was not observed. This might be the result of other regulatory mechanisms for this protein. It has been documented that the regulation of maize NR is dependent on both gene expression as well as protein phosphorylation (31).

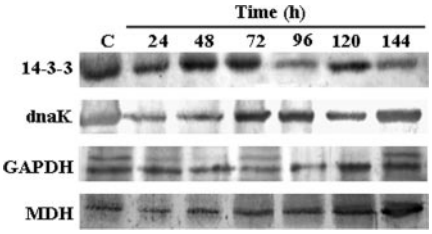

FIG. 7. **Immunoblot analysis for few of the representative DRPs.** The nuclear expression profile for 14-3-3, dnaK, GAPDH, and MDH was detected using one-dimensional Western blot analysis; 100 μg of nuclear protein for all seven time points was separated by 12.5% SDS-PAGE and blotted onto Hybond-C membrane. The blots were probed with respective primary antibodies and signal detected.

DISCUSSION

Within the larger goal of profiling protein expression in plant under dehydration, the aim of this study was to characterize the regulatory and functional pathways operating in chickpea nucleus. A model representing the regulatory and functional network activated under dehydration is depicted in Fig. 9. Proteins of the regulatory network include transcription factors, RNA-binding proteins, protein kinases, and phosphatases (4, 32–33). The functional network comprises proteins whose activity enables the plant to survive stress conditions and includes proteins involved in ion homoeostasis (34), water channels (35), enzymes involved in scavenging of ROS (36), enzymes involved in the synthesis of osmolytes and compatible solutes (37), and protective proteins (38).

Dehydration Responsive Regulatory Network in Nucleus—The nucleus is the site where the genetic material is transcribed into mRNAs, which carry the blueprint to synthesize proteins. Because the protein synthesis is a very complicated and highly regulated process, many different proteins are needed to ensure that a gene is transcribed at the right time in the life of a cell. This indicates that a lot of molecules have to get in and out of the nucleus at any given time. The major regulator in this transport is an intracellular signaling protein called Ran (CaN-347), which stands for *Ra*s-related protein in the *n*ucleus. The small Ras-like GTPase Ran was highly upregulated under dehydration (Table II). This protein is known to play a crucial role in nucleocytoplasmic transport in that it

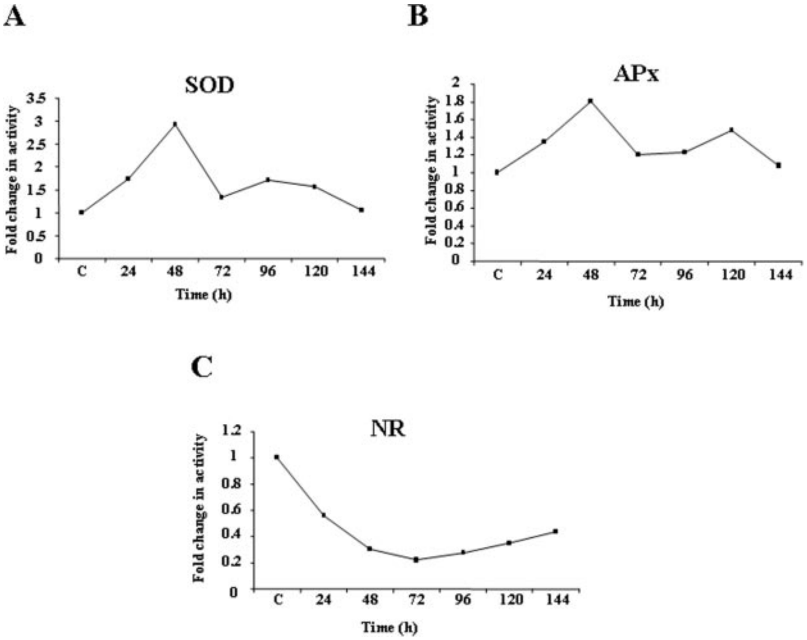

FIG. 8. **Monitoring enzymatic activities of SOD, APx, and NR under dehydration in chickpea nucleus.** The enzymes viz., SOD (*A*), APx (*B*), and NR (*C*) were extracted and the activities were assayed as described under "Experimental Procedures." Enzyme activities are expressed in terms of fold change over the seven dehydration time points studied.

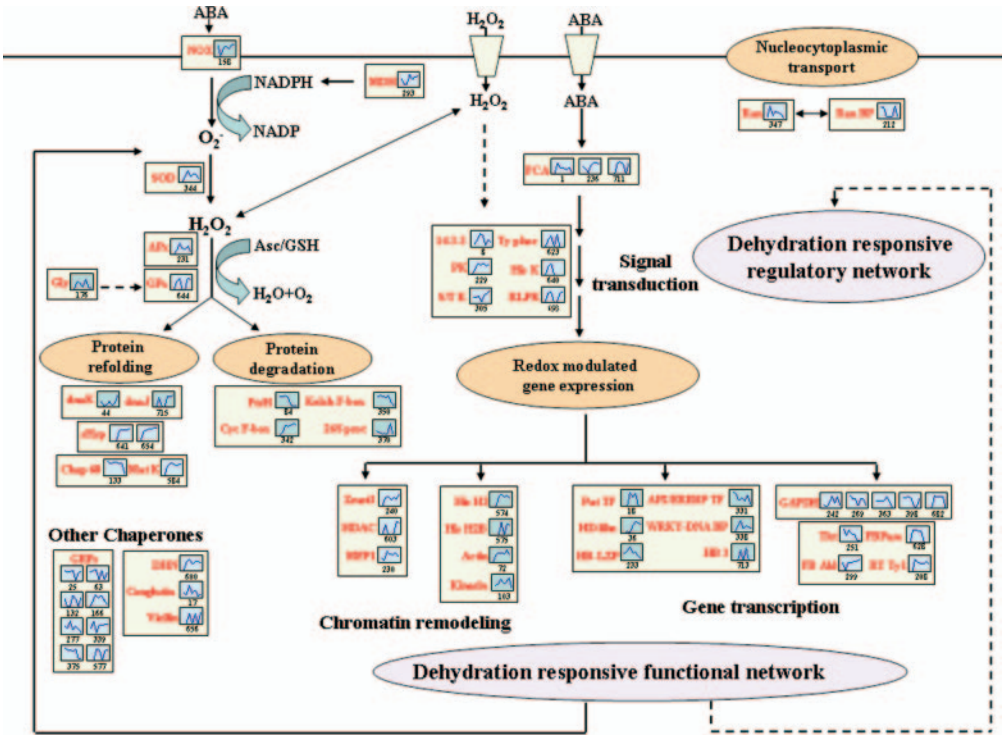

FIG. 9. **The regulatory and the functional network activated under dehydration stress in chickpea nucleus.** Proteins identified in this study are indicated in the *box. Graphs* are representative of expression profiles of individual protein; the number given below in each *graph* indicates the protein identification number. Abbreviations for metabolites: *NOX*, NADPH oxidase; Gly, glyoxalase; *Chap 60*, chaperonin 60; *Mat K*, maturase K; *Cyc F-box*, cyclin like F-box; *26S prot*, 26S proteasome subunit; *PK*, protein kinase; *S/T K*, serine/threonine kinase; *Ty phos*, tyrosine phosphatase; *His K*, histidine kinase; *RLPK*, receptor-like protein kinase; *DHN*, dehydrin; *Zmet3*, DNA cytosine methyltransferase; *MFP1*, MAR binding filament-like protein 1; *His H3*, histone H3; *His H2B*, histone H2B; *Put TF*, putative transcription factor; *HD-like*, homeodomain-like; *HB-LZP*, homeobox-leucine zipper protein; *AP2/EREBP TF*, AP2/EREBP transcription factor BABY BOOM; *WRKY-DNA BP*, WRKY-DNA binding protein; *HB3*, homeobox protein 3; *Tkt*, transketolase; *FB Ald*, fructose biphosphate aldolase; *RT Ty 1*, retrotransposon Ty1-copia subclass.

provides the identity of the two compartments and thus ensures directionality of transport (39). The cytoplasmic fibrils of the nuclear pore consist of a very large molecule called RanBP (CaN-212), for Ran-Binding protein. It is thought that the function of RanBP is to watch out for Ran-cargo complexes coming out of the nuclear pore (40). 14-3-3 protein (CaN-8) is also involved in the nucleocytoplasmic transport (41); however, we have included this protein as a part of signal transduction because it is known to have a number of interacting protein partners.

Several proteins involved in early stress responsive signaling were identified in this study. Dehydration is known to induce abscisic acid (ABA) in the stressed cells. It has been documented that ABA can cause an increased generation of O_2^- (42) and H_2O_2 (43, 44), and induce the expression and activity of antioxidant genes (42, 45, 46). FCA (CaN-1, 236, 711) is a known ABA receptor in nucleus of higher plants (47), which might be involved in this signaling network even though it may correspond to a degradation product as is evident from its gel-based molecular weight. However, there is not much information on the downstream elements of this pathway. Signaling partners like 14-3-3 (CaN-8), protein kinase (CaN-229), serine-threonine kinase (CaN-305), histidine kinase (CaN-640), receptor-like protein kinase (CaN-693) and tyrosine phosphatase (CaN-623) might be involved in relaying this signal to the heterochromatin region so as to regulate gene expression. While all of these signaling partners were early dehydration responsive (up-regulated as early as 24 h), serine-threonine kinase was up-regulated only after 96 h (Table II). Recently, it has been shown that tobacco cells transformed with an antisense construct of 14-3-3 no longer accumulate ROS (48) suggesting 14-3-3 protein as a very important component in this signaling pathway. NR (CaN-710) is known to catalyze a one electron transfer from NADPH to nitrite to produce nitric oxide (NO) (49, 50), a potential signaling intermediate (51). Dehydration stress causes increased NR protein turnover and accelerated mRNA turnover (30, 52) and 14-3-3 proteins are instrumental in bringing about this degradation. The availability of 14-3-3s for binding to phosphorylated-NR controls the stability of NR via proteolysis (53), which explains the concomitant rise in degraded NR levels along with the rise in 14-3-3 protein levels (Table II).

Stress-mediated effects on chromatin remodeling are well established in yeast. Histone deacetylase (HDAC; CaN-603) interacts with the 14-3-3 family of proteins that are known to bind specifically to conserved phosphoserine-containing motifs. 14-3-3 proteins negatively regulate HDAC by preventing its nuclear localization and thereby uncovering a novel regulatory mechanism for HDACs (54). Alternatively, association with 14-3-3 proteins may stimulate the nuclear export of HDAC and might account for the decrease in HDAC protein level after 48 h and subsequent increase after 120 h when 14-3-3 levels go down (Table II). DNA cytosine methyltransferase Zmet3 (CaN-240) was found to be consistently up-regulated following dehydration stress. DNA methylation and histone deacetylation work in combination to regulate gene transcription (55, 56). High methylcytosine contents and low histone acetylation are frequently associated with silent genes. Matrix or scaffold attachment regions (MARs or SARs) are involved in looping of open chromatin fibers. The interaction of chromatin with the nuclear matrix via MARs on the DNA is considered to be of fundamental importance for higher order chromatin organization and regulation of gene expression. MARs have a positive effect on gene expression (57, 58) and MAR binding filament-like protein 1 (MFP1; CaN-230) with a filament protein-like structure is a good candidate for a MAR binding constituent of the nuclear filaments (59).

H1 histone has long been known to be induced by water-deficit (60). We found that histones H3 (CaN-574) and H2B (CaN-575) were continuously induced after 48 h of dehydration. The up-regulation of histones might be involved in controlling downstream gene expression during dehydration stress. Actin (CaN-72) is not only a major cytoskeletal component in all eukaryotic cells but also a nuclear protein that plays a role in gene transcription (61). Actin's functional complexity makes it a likely target of oxidative stress. 14-3-3 proteins may contribute to the reorganization of the actin cytoskeleton by interacting with actin-depolymerizing factor protein (62). Kinesin (CaN-103), a microtubule-dependent ATPase, is also thought to be a part of this machinery and was found to be differentially regulated by dehydration stress.

The differential proteome of chickpea nucleus also revealed the presence of a number of glycolytic pathway enzymes. All of these proteins are known to have nonglycolytic function in the nucleus. GAPDH (CaN-242, 269, 363, 398, 682) has been proposed to act as a tRNA-binding protein and may participate in RNA export (63). All five isoforms of this protein showed a different expression profile. Aldolase (CaN-299), on the other hand, was initially identified as a DNA-binding protein when it was purified from SEWA sarcoma cells of vertebrate species (64). The phosphorylation of fructose-bisphosphatase (FBPase) (CaN-628) might be the signal inducing the movement of the enzyme to the nucleus where it might induce the expression of its own gene, although a possibility that FBPase influences the expression of other genes cannot be ruled out (65). Transketolase (CaN-251), another enzyme of the same pathway, was also found to be differentially regulated under dehydration stress. Retrotransposons have been shown to be specifically activated by environmental stress signaling (66), which was again corroborated by our results showing a constant increase in the protein levels as early as after 24 h of dehydration.

Numerous studies have shown that transcription factors are important in regulating plant responses to environmental stress. Different members of transcription factors regulate the gene expression in response to dehydration stress. However, many of these would have escaped detection as the expression level for transcription factors is generally not very high. The AP2/EREBP transcription factor BABY BOOM (CaN-331), involved in plant growth and development (67), was found to be completely shutdown under dehydration. Other transcription factors identified in this study are homeobox-leucine zipper protein (CaN-233), homeobox protein HB3 (CaN-713), putative transcription factor (CaN-18), and WRKY-DNA binding domain protein (CaN-338), all of which showed an up-regulation. The exact function of these proteins can only be predicted after extensive studies, and might be interesting for future investigations.

Dehydration Responsive Functional Network in Nucleus—Whether ABA acts upstream of ROS or vice-versa is controversial as gene expression via ROS-independent ABA signaling is also common in plants. NADPH oxidase (CaN-158), a so-called "respiratory burst oxidase homologue" mediating ABA induced ROS (68), are known nuclear membrane proteins that may produce O_2^- in the vicinity of membrane ion channels (69). The resulting oxidative species, in turn, act as secondary messengers to control a variety of physiological responses. It is clear that this "respiratory burst" must have an adequate supply of NADPH for ROS generation, which suggests that a transient increase in NADP(H) is a requirement for this signaling pathway (70). The required NADPH for this reaction might be generated by MDH (CaN-293), making it an important member of the ROS pathway (71). Both NADPH oxidase and MDH were down-regulated under dehydration, but their accumulation showed a slight increase around 120 h. Although ROS is necessary for signaling and stress-induced gene expression, excess ROS can cause damage to proteins, DNA, and lipids in the cell. Thus, removal of excess free radicals from the cell is necessary through specific detoxification mechanisms. SOD (CaN-344) constitutes the first line of defense against ROS, thereby converting O_2^- to H_2O_2. APx (CaN-231) and GPx (CaN-644) in turn act in parallel to convert the peroxide ion into molecular oxygen and water. Even though APx and GPx have not been reported in plant nucleus, their presence in animal nuclei (72, 73) is known. Methylglyoxal has a binding site on GPx, and its high levels inhibit enzyme activity (74). Since GPx catalyzes the detoxification of H_2O_2, its inactivation leads to the accumulation of ROS. Glyoxalase (CaN-176) carry out catabolism of methylglyoxal and is indirectly involved in scavenging ROS (75). 2-cys peroxiredoxins (CaN-6) are a large family of peroxidases, which reduce alkyl hydroperoxides and hydrogen peroxide. Although they are known chloroplastic enzymes, PER1 is one of the first enzymatic plant antioxidants found to be localized in the nucleus (76).

The ROS-mediated proteolytic degradation might be executed by kelch repeat-containing F-box family protein (CaN-350), putative FtsH-like protein Pftf (CaN-84), and ATP-dependent 26S proteasome (CaN-370). Because intact proteins are less sensitive to oxidation than misfolded proteins (77), the protein chaperones get up-regulated in response to stresses. Different chaperones are documented to play complementary, and sometimes overlapping, roles in protection of proteins. The dnaK (CaN-644), an Hsp70-like protein chaperone together with its co-chaperones dnaJ (CaN-715) and GrpE constitutes the KJE system and prevents aggregation of misfolded proteins, thus facilitating their subsequent refolding (78). The small heat shock proteins (sHsps; CaN-641 and 654) are proposed to bind unfolding proteins, providing a reservoir of substrates available for subsequent refolding by the KJE system (79). Redox sensitive molecular targets usually contain highly conserved cysteine residues, and their oxidation, nitration, and formation of disulfide links are crucial events in oxidant/redox signaling. ROS has also been shown to cause increased gene expression of stress response genes (HSP-27, 70, and 90) and antioxidant enzymes (APx, SOD, GPx), mediated or regulated by redox-sensitive transcription factors (such as NF-κB and AP-1) (80). Protein translation may represent another way of combating dehydration, which explains the initial increase in protein levels for translation elongation factor (CaN-218 and 345) even though it shows a complete down-regulation after 72 h.

Dehydrins (CaN-600), which are also known as late-embryogenesis-abundant protein group II, have been most extensively studied in relation to drought and cold stresses (81, 82). Dehydrins have been proposed to have a protective function during abiotic stress via a number of different mechanisms. These include improving or protecting enzyme activity under cold or dehydration conditions (83, 84); or acting as radical scavengers (85) or as membrane stabilizers (81, 86). Vicilin (CaN-656) and conglutin (CaN-17) are basically storage proteins, which possess a lectin-type activity. However, there is a report that a pea nuclear protein belonging to the vicilin superfamily gets accumulated under dehydration stress (87). As the protein was shown to share homology with dehydrins, it was suggested that the function of this protein may be related to the protection of chromatin structure against desiccation. Another protein with a chaperone-like activity was the class of glycine-rich RNA binding proteins (GRPs; CaN-25, 63, 132, 166, 277, 339, 375, and 577). These proteins were identified from different parts of the two-dimensional electrophoresis gel representing different molecular weight and pI, which is fairly surprising. The GRPs are RNA chaperones, and have been shown to be responsive to environmental stresses in particular, cold stress (88).

Dehydration stress also showed differential response for a number of ATPases (CaN-105, 135, 235, 298, 353, and 660), glycine dehydrogenase protein (CaN-402), and phenylcoumarin benzylic ether reductase or isoflavone reductase (PCBER/IFR; CaN-291, 369, and 674). PCBER/IFR is involved in secondary metabolism and plays an important role in plant defense (89). As many as 26 proteins with no known function were also identified in chickpea nucleus. The prediction of a possible function for these proteins under dehydration would make up an interesting study.

In conclusion, we have investigated the molecular responses to dehydration stress in chickpea at nuclear-specific proteome level and identified the probable DRPs that play a variety of cellular functions.

---

* This research work was supported by grants from the Department of Biotechnology, Ministry of Science and Technology, India and the National Institute for Plant Genome Research (to N. C.) and by a predoctoral fellowship (to A. P.) from the Council of Scientific and Industrial Research, Government of India. The costs of publication of this article were defrayed in part by the payment of page charges. This article must therefore be hereby marked "*advertisement*" in accordance with 18 U.S.C. Section 1734 solely to indicate this fact.

S The on-line version of this article (available at http://www.mcponline.org) contains supplemental material.

‡ To whom correspondence may be addressed: National Institute for Plant Genome Research, Aruna Asaf Ali Marg, New Delhi-110067, India. Tel.: 91-11-26735186; Fax: 91-11-26716658; E-mail: subhrac@hotmail.com.

§ To whom correspondence may be addressed: National Institute for Plant Genome Research, Aruna Asaf Ali Marg, New Delhi-110067, India. Tel.: 91-11-26735178; Fax: 91-11-26716658; E-mail: nchakraborty@hotmail.com.

REFERENCES

1. Araus, J. L., Slafer, G. A., Reynolds, M. P., and Royo, C. (2002) Plant breeding and drought in C-3 cereals: what should we breed for? *Ann. Bot.* **89,** 925–940
2. Boyer, J. S. (1982) Plant productivity and environment. *Science*, **218,** 443–448
3. McKersie, B. D., and Leshem, Y. Y. (1994) Desiccation in *Stress and Stress Coping in Cultivated Plants* (McKcKersie, B. D., and Leshem, Y. Y., eds), pp. 132–144 Kluwer, Dordrechet, The Netherlands
4. Shinozaki, K., and Yamaguchi-Shinozaki, K. (2000) Molecular responses to dehydration and low temperature: differences and cross-talk between two stress signaling pathways. *Curr. Opin. Plant Biol.* **3,** 217–223
5. Chandler, P. M., and Robertson, M. (1994) Gene expression regulated by abscisic acid and its relation to stress tolerance. *Annu. Rev. Plant Physiol. Plant Mol. Biol.* **45,** 113–141
6. Ouvrard, O., Cellier, F., Ferrare, K., Tousch, D., Lamaze, T., Dupuis, J. M., and Casse-Delbart, F. (1996) Identification and expression of water stress- and abscisic acid-regulated genes in a drought-tolerant sunflower genotype. *Plant Mol. Biol.* **31,** 819–829
7. Riccardi, F., Gazeau, P., Vienne, D.V., and Zivy, M. (1998) Protein changes in responses to progressive water deficit in maize. *Plant Physiol.* **117,** 1253–1263
8. Bray, E. A. (1993) Molecular responses to water deficit. *Plant Physiol.* **103,** 1035–1040
9. Seki, M., Narusaka, M., Ishida, J., Nanjo, T., Fujita, M., Oono, Y., Kamiya, A., Nakajima, M., Enju, A., Sakurai, T., Satou, M., Akiyama, K., Taji, T., Yamaguchi-Shinozaki, K., Carninci, P., Kawai, J., Hayashizaki, Y., and Shinozaki, K. (2002) Monitoring the expression profiles of 7000 Arabidopsis genes under drought, cold and high-salinity stresses using a full-length cDNA microarray. *Plant J.* **31,** 279–292
10. Shinozaki, K., and Yamaguchi-Shinozaki, K. (1997) Gene expression and signal transduction in water-stress response. *Plant Physiol.* **115,** 327–334

11. Tian, Q., Stepaniants, S. B., Mao, M., Weng, L., Feetham, M. C., Doyle, M. J., Yi, E. C., Dai, H. Y., Thorsson, V., Eng, J., Goodlett, D., Berger, J. P., Gunter, B., Linseley, P. S., Stoughton, R. B., Aebersold, R., Collins, S. J., Hanlon, W. A., and Hood, L. E. (2004) Integrated genomic and proteomic analyses of gene expression in mammalian cells. *Mol. Cell. Proteomics* **3,** 960–969
12. Gygi, S. P., Rochon, Y., Franza, B. R., and Aebersold, R. (1999) Correlation between protein and mRNA abundance in yeast. *Mol. Cell. Biol.* **19,** 1720–1730
13. Westbrook, J. A., Wheeler, J. X., Wait, R., Welson, S. Y., and Dunn, M. J. (2006) The human heat proteome: 2D maps using narrow range immobilised pH gradients. *Electrophoresis* **27,** 1547–1555
14. Dreger, M. (2003) Proteome analysis at the level of subcellular structures. *Eur. J. Biochem.* **270,** 589–603
15. Bhushan, D., Pandey, A., Chattopadhyay, A., Choudhary, M. K., Chakraborty, S., Datta, A., and Chakraborty, N. (2006) Extracellular matrix proteome of chickpea (*Cicer arietinum* L.) illustrates pathway abundance, novel protein functions and evolutionary perspect. *J. Proteome Res.* **5,** 1711–1720
16. Pandey, A., Choudhary, M. K., Bhushan, D., Chatttopadhyaya, A., Chakraborty, S., Datta, A., and Chakraborty, N. (2006) The nuclear proteome of chickpea reveals predicted and unexpected proteins. *J. Prot. Res.* **5,** 3301–3311
17. Hulse, J. H. (1991) Nature, composition and utilization of grain legumes. p. 11–27. In: Uses of tropical Legumes: Proceedings of a Consultants' Meeting, 27–30 March 1989, ICRISAT Center. ICRISAT, Patancheru, A.P. 502 324, India.
18. Casey, T. M., Arthur, P. G., and Bogoyevitch, M. A. (2005) Proteomic analysis reveals different protein changes during endothelin-1- or leukemic inhibitory factor-induced hypertrophy of cardiomyocytes in vitro. *Mol. Cell. Proteomics* **4***,* 651–661
19. Romijin, E. P., Christis, C., Wieffer, M., Gouw, W. J., Fullaondo, A., Sluijs, P., Braakman, I., and Heck, A. J. R. (2005) Expression clustering reveals detailed co-expression patterns of functionally related proteins during B cell differentiation. *Mol. Cell. Proteomics* **4,** 1297–1310
20. Paoletti, F., Aldinucci, D., Mocali, A., and Caparrini, A. (1986) A sensitive spectrophotometric method for the determination of superoxide dismutase activity in tissue extracts. *Anal. Biochem.* **154,** 538–541
21. Nakano, Y., and Asada, K. (1981) Hydrogen peroxide is scavenged by ascorbate-specific peroxidase in spinach chloroplasts. *Plant Cell Physiol.* **22,** 867–880
22. Gilliam, M. B., Sherman, M. P., Griscavage, J. M., and Ignarro, L. J. (1993) A spectrophotometric assay for nitrate using NADPH oxidation by aspergillus nitrate reductase. *Anal. Biochem.* **212,** 359–365
23. Cherian, M., Smith, J. B., Jiang, X. Y., and Abraham, E. C. (1997) Influence of protein glutathione mixed disulfide on the chaperone-like function of alpha-crystallin. *J. Biol. Chem.* **272,** 29099–29103
24. Colvis, C., and Garland, D. (2002) Posttranslational modification of human alphaA-crystallin: correlation with electrophoretic migration. *Arch. Biochem. Biophys.* **397***,* 319–323
25. Hanson, S. R. A., Hasan, A, Smith, D. L., and Smith, J. B. (2000) The major in vivo modifications of the human water-insoluble lens crystallins are disulfide bonds, deamidation, methionine oxidation and backbone cleavage. *Exp. Eye Res.* **71,** 195–207
26. Ueda, Y., Duncan, M. K., and David, L. L. (2002) Lens proteomics: the accumulation of crystallin modifications in the mouse lens with age. *Invest. Ophthalmol. Vis. Sci.* **43,** 205–215
27. Apel, K., and Hirt, H. (2004) Reactive oxygen species: metabolism, oxidative stress, and signal transduction. *Annu. Rev. Plant Biol.* **55,** 373–399
28. Papadakis, A. K., and Roubelakis-Angelakis, K. A. (2005) Polyamines inhibit NADPH oxidase-mediated superoxide generation and putrescine prevents programmed cell death induced by polyamine oxidase-generated hydrogen peroxide. *Planta* **220,** 826–837
29. Fridovich, I. (1986) Superoxide dismutases. *Advances Enzymol. Related Areas Mol. Biol.* **58,** 61–97
30. Foyer, C. H., Valadier, M. H., Migge, A., and Becker, T. W. (1998) Drought-induced effects on nitrate reductase activity and mRNA and on the coordination of nitrogen and carbon metabolism in maize leaves. *Plant Physiol.* **117,** 283–292
31. Huber, J. L., Redinbaugh, M. G., Huber, S. C., and Campbell, W. H. (1994) Regulation of maize leaf nitrate reductase activity involves both gene expression and protein phosphorylation. *Plant Physiol.* **106,** 1667–1674
32. Rock, C. D. (2000) Pathways to abscisic acid-regulated gene expression. *New Phytol.* **148,** 357–396
33. Xiong, L., and Zhu, J. K. (2001) Abiotic stress signal transduction in plants: molecular and genetic perspectives. *Physiol. Plantarum* **112,** 152–166
34. Blumwald, E. (2000) Sodium transport and salt tolerance in plants. *Curr. Opin. Cell Biol.* **12,** 431–434
35. Johansson, I., Karlsson, M., Johanson, U., Larsson, C., and Kjellbom, P. (2000) The role of aquaporins in cellular and whole plant water balance. *Biochim. Biophys. Acta* **1465,** 324–342
36. Bohnert, H. J., and Sheveleva, E. (1998) Plant stress adaptations: making metabolism move. *Curr. Opin. Plant Biol.* **1,** 267–274
37. Bohnert, H. J., and Shen, B. (1999) Transformation and compatible solutes. *Sci. Hortic.* **78,** 237–260
38. Hasegawa, P. M., Bressan, R. A., Zhu, J. K., and Bonhert, H. J. (2000) Plant cellular and molecular responses to high salinity. *Annu. Rev. Plant Physiol. Plant Mol. Biol.* **51,** 463–499
39. Melchior, F., and Gerace, L. (1998) Two-way trafficking with Ran. *Trends Cell. Biol.* **8,**175–179
40. Vetter, I. R., Nowak, C., Nishimoto, T., Kuhlmann, J., and Wittinghofer, A. (1999) Structure of a Ran-binding domain complexed with Ran bound to a GTP analogue: implications for nuclear transport. *Nature* **398,** 39–46
41. Brunet, A., Kanai, F., Stehn, J., Xu, J., Sarbassova, D., Frangioni, J. V., Dalal, S. N., DeCaprio, J. A., Greenberg, M. E., and Yaffe, M. B. (2002) 14-3-3 transits to the nucleus and participates in dynamic nucleocytoplasmic transport. *J. Cell Biol.* **156,** 817–828
42. Jiang, M., and Zhang, J. (2001) Effect of abscisic acid on active oxygen species, antioxidative defence system and oxidative damage in leaves of maize seedlings. *Plant Cell Physiol.* **42,** 1265–1273
43. Guan, L., Zhao, J., and Scandalios, J. G. (2000) Cis-elements and trans-factors that regulate expression of the maize Cat1 antioxidant gene in response to ABA and osmotic stress: H_2O_2 is the likely intermediary signalling molecule for the response. *Plant J.* **22,** 87–95
44. Zhang, X., Zhang, L., Dong, F., Gao, J., Galbraith, D. W., and Song, C. P. (2001) Hydrogen peroxide is involved in abscisic acid-induced stomatal closure in *Vicia faba*. *Plant Physiol.* **126,** 1438–1448
45. Bueno, P., Piqueras, A., Kurepa, J., Savoure, A., Verbruggen, N., Van Montagu, M., and Inze, D. (1998) Expression of antioxidant enzymes in response to abscisic acid and high osmoticum in tobacco BY-2 cell cultures. *Plant Sci.* **138,** 27–34
46. Anderson, M. D., Prasad, T. K., Martin, B. A., and Stewart, C. R. (1994) Differential gene expression in chilling-acclimated maize seedlings and evidence for the involvement of abscisic acid in chilling tolerance. *Plant Physiol.* **105,** 331–339
47. Razem, F. A., El-Kereamy, A., Abrams, S. R., and Hill, R. D. (2006) The RNA-binding protein FCA is an abscisic acid receptor. *Nature* **439,** 290–294
48. Elmayan, T, Fromentin, J, Riondet, C, Alcaraz, G, Blein, J. P., and Simon-Plas, F. (2007) Regulation of reactive oxygen species production by a 14-3-3 protein in elicited tobacco cells. *Plant, Cell Environ.* **30,** 722–732
49. Dean, J. V., and Harper, J. E. (1988) The conversion of nitrite to nitrogen oxide(s) by the constitutive NAD(P)H-nitrate reductase enzyme from soybean. *Plant Physiol.* **88,** 389–395
50. Yamasaki, H., Sakihama, Y., and Takahashi, S. (1999) An alternative pathway for nitric oxide production in plants: new features for an old enzyme. *Trends Plant Sci.* **4,** 128–129
51. Wendehenne, D., Durner, J., and Klessig, D. F. (2004) Nitric oxide: a new player in plant signalling and defence responses. *Curr. Opin. Plant Biol.* **7,** 449–455
52. Ferrario-Mery, S., Valadier, M. H., and Foyer, C. H. (1998) Overexpression of nitrate reductase in tobacco delays drought-induced decreases in nitrate reductase activity and mRNA. *Plant Physiol.* **117,** 293–302
53. Weiner, H., and Kaiser, W. M. (1999) 14-3-3 proteins control proteolysis of nitrate reductase in spinach leaves. *FEBS Lett.* **455,** 75–78
54. Grozinger, C. M., and Schreiber, S. L. (2000) Regulation of histone deacetylase 4 and 5 and transcriptional activity by 14-3-3-dependent cellular localization. *Proc. Natl. Acad. Sci. U. S. A.* **97,** 7835–7840
55. Dobosy, J. R., and Selker, E. U. (2001) Emerging connections between DNA methylation and histone acetylation. *Cell Mol. Life Sci.* **58,** 721–727
56. Loidl, P. (2004) A plant dialect of the histone language. *Trends Plant Sci.* **9,** 84–90

57. Allen, G. C., Hall, G. E. J., Michalowski, S., Newman, W., Spiker, S., Weissinger, A. K., and Thompson, W. F. (1996) High-level transgene expression in plant cells: effects of a strong scaffold attachment region from tobacco. *Plant Cell* **8,** 899–913
58. Mlynárová Keizer, L. C. P., Stiekema, W. J., and Nap, J. P. (1996) Approaching the lower limits of transgene variability. *Plant Cell* **8,** 1589–1599
59. Gindullis, F., and Meier, I. (1999) Matrix attachment region binding protein MFP1 is localized in discrete domains at the nuclear envelope. *Plant Cell*, **11,** 1117–1128
60. Wei, T., and O'Connell, M. A. (1996) Structure and characterization of a putative drought-inducible H1 histone gene. *Plant Mol. Biol.* **30,** 255–268
61. Percipalle, P., and Visa, N. (2006) Molecular functions of nuclear actin in transcription. *J. Cell Biol.* **172,** 967–971
62. Gohla, A., and Bokoch, G. M. (2002) 14-3-3 regulates actin dynamics by stabilizing phosphorylated cofilin. *Curr. Biol.* **12,** 1704–1710
63. Singh, R., and Green, M. R. (1993) Sequence-specific binding of transfer RNA by glyceraldehyde-3-phosphate dehydrogenase. *Science* **259,** 365–368
64. Ronai, Z., Robinson, R., Rutberg, S., Lazarus, P., and Sardana, M. (1992) Aldolase DNA interactions in a SEWA cell system. *Biochim. Biophys. Acta* **1130,** 20–28
65. Gizak, A., and Dzugaj, A. (2003) FBPase is in the nuclei of cardiomyocytes. *FEBS Lett.* **539,** 51–55
66. Grandbastien, M. A. (1998) Activation of plant retrotransposons under stress conditions. *Trends Plant Sci.* **3,** 181–187
67. Boutilier, K., Offringa, R., Sharma, V. K., Kieft, H., Ouellet, T., Zhang, L., Hattori, J., Liu, C. M., van Lammeren, A. A. M., Miki, B. L. A., Custers, J. B. M., and van Lookeren Campagne, M. M. (2002) Ectopic expression of BABY BOOM triggers a conversion from vegetative to embryonic growth. *Plant Cell* **14,** 1737–1749
68. Neill, S. J., Desikan, R., Clarke, A., Hurst, R. D., and Hancock, J. T. (2001) Hydrogen peroxide and nitric oxide as signalling molecules in plants. *J. Exp. Bot.* **53,** 1237–1244
69. Ushio-Fukai, M. (2006) Localizing NADPH oxidase-derived ROS. *Sci. STKE* 2006, re8
70. Harding, S. A., Oh, S. H., and Roberts, D. M. (1997) Transgenic tobacco expressing a foreign calmodulin gene shows an enhanced production of active oxygen species. *EMBO J.* **16,** 1137–1144
71. Gross, G. G., Janse, C., and Elstner, E. F. (1977) Involvement of malate, monophenols and superoxide radical in hydrogen peroxide formation by isolated cell walls from horseradish (*Armoracia lapathifolia Gilib*). *Planta* **136,** 271–276
72. Asayama, K., Yokota, S., Dobashi, K., Kawada, Y., Nakane, T., Kawaoi, A., and Nakazawa, S. (1996) Immunolocalization of cellular glutathione peroxidase in adult rat lungs and quantitative analysis after postembedding immunogold labeling. *Histochem. Cell Biol.* **105,** 383–389
73. Komatsu, H., Okayasu, I., Mitomi, H., Imai, H., Nakagawa, Y., and Obata, F. (2001) Immunohistochemical detection of human gastrointestinal glutathione peroxidase in normal tissues and cultured cells with novel mouse monoclonal antibodies. *J. Histochem. Cytochem.* **49,** 759–766
74. Park, Y. S., Koh, Y. H., Takahashi, M., Miyamoto, Y., Suzuki, K., Dohmae, N., Takio, K., Honke, K., and Taniguchi, N. (2003) Identification of the binding site of methylglyoxal on glutathione peroxidase: methylglyoxal inhibits glutathione peroxidase activity via binding to glutathione binding sites Arg 184 and 185. *Free Radic. Res.* **37,** 205–211
75. Singla-Pareek, S. L., Reddy, M. K., and Sopory, S. K. (2003) Genetic engineering of the glyoxalase pathway in tobacco leads to enhanced salinity tolerance. *Proc. Natl. Acad. Sci. U. S. A.* **100,** 14672–14677
76. Stacy, R. A. P., Nordeng, T. W., Culianez-Macia, F. A., and Aalen, R. B. (1999) The dormancy-related peroxiredoxin anti-oxidant, PER1, is localized to the nucleus of barley embryo and aleurone cells. *Plant J.* **19,** 1–8
77. Berlett, B. S., Levine, R. L., and Stadtman, E. R. (1996) Comparison of the effects of ozone on the modification of amino acid residues in glutamine synthetase and bovine serum albumin. *J. Biol. Chem.* **271,** 4177–4182
78. Mogk, A., Tomoyasu, T., Goloubinoff, P., Rudiger, S., Roder, D., Langen, H., and Bukau, B. (1999) Identification of thermolabile E. coli proteins: prevention and reversion of aggregation by DnaK and C1pB. *EMBO J.* **18,** 6934–6949
79. Narberhaus, F. (2002) α-Crystallin-type heat shock proteins: socializing minichaperones in the context of a multichaperone network. *Microbiol. Mol. Biol. Rev.* **66,** 64–93
80. Rahman, I. (2003) Oxidative stress, chromatin remodeling and gene transcription in inflammation and chronic lung diseases. *J. Biochem. Mol. Biol.* **36,** 95–109
81. Close, T. J. (1996) Dehydrins: emergence of a biochemical role of a family of plant dehydration proteins. *Physiol. Plant* **97,** 795–803
82. Close, T. J. (1997) Dehydrins: a commonality in the response of plants to dehydration and low temperature. *Physiol. Plant* **100,** 291–296
83. Rinne, P. L. H., Kaikuranta, P. L. M., van der Plas, L. H. W., and van der Shoot, C. (1999) Dehydrins in cold acclimation apices of birch (*Betula pubescens* Ehrh.): production, localization and potential role in rescuing enzyme function during dehydration. *Planta*, **209,** 377–388
84. Sanchez-Ballesta, M. T., Rodrigo, M. J., Lafuente, M. T., Granell, A., and Zacarias, L. (2004) Dehydrin from citrus, which confers *in vitro* dehydration and freezing protection activity, is constitutive and highly expressed in the flavedo of fruit but responsive to cold and water stress in leaves. *J. Agric. Food Chem.* **52,** 1950–1957
85. Hara, M., Terashima, T. F., Fukaya, T., and Kuboi, T. (2003) Enhancement of cold tolerance and inhibition of lipid peroxidation by citrus dehydrin in transgenic tobacco. *Planta* **217,** 290–298
86. Koag, M. C., Fenton, R. D., Wilkens, S., and Close, T. J. (2003) The binding of maize DHN1 to lipid vesicles: gain of structure and lipid specificity. *Plant Physiol.* **131,** 309–316
87. Castillo, J., Rodrigo, M. I., Marquez, J. A., Zuniga, A., and Franco, L. (2000) A pea nuclear protein that is induced by dehydration belongs to the vicilin superfamily. *Eur. J. Biochem.* **267,** 2156–2165
88. Carpenter, C. D., Kreps, J. A., and Simon, A. E. (1994) Genes encoding glycine-rich *Arabidopsis thaliana* proteins with RNA-binding motifs are influenced by cold treatment and an endogenous circadian rhythm. *Plant Physiol.* **104,** 1015–1025
89. Gang, D. R., Kasahara, H., Xia, Z. Q., Mijnsbrugge, K. V., Bauw, G., Boerjan, W., van Montagu, M., Davin, L. B., and Lewis, N. G. (1999) Evolution of plant defense mechanisms. *J. Biol. Chem.* **274,** 7516–7527